

Supramolecular Structure of the LiPFN–PVP System: ^{19}F NMR Studies

Anna Laura Segre and Noemi Proietti

*Istituto di Strutturistica Chimica e Servizio NMR Area della Ricerca del CNR, Caselle,
Postale 10, 00016 Monterotondo Stalione, Roma, Italia*

Bianca Sesta* and Alessandro D'Aprano

Dipartimento di Chimica, Università La Sapienza P.le A. Moro 5 00185 Roma, Italia

Maria Emanuela Amato

Dipartimento di Chimica, Università di Catania, Viale Andrea Doria 6, 95125 Catania, Italia

Received: June 26, 1998

^{19}F NMR measurements on lithium perfluorononanoate [LiPFN] in D_2O and in solutions of D_2O with poly(vinylpyrrolidone) [PVP] at different molecular weights have been carried out. A careful study of literature data and COSY maps allowed the full assignment of the ^{19}F resonances as a function of concentration and composition of the systems. For the LiPFN/ D_2O system, analysis of the chemical shifts of the fluorine atoms bound to the different carbons of the LiPFN backbone reveals significant variations correlated to the LiPFN concentration. Such a finding has been explained in terms of the changes in the local dielectric constant caused by the surfactant self-aggregation process. The presence of PVP in solution strongly modifies the trend of the ^{19}F chemical shifts observed in the binary LiPFN/ D_2O system. Such a feature, depending both on the position of the fluorine atoms along the surfactant backbone and on the LiPFN concentration, indicates the presence of strong polymer–surfactant interactions. The line width analysis of selected ^{19}F resonances as a function of the surfactant concentration shows, in addition, the presence of an equilibrium among different species of LiPFN in solution (i.e., free monomers, bound monomers, free micelles, bound micelles). The extreme spread of ^{19}F chemical shifts allow the spectroscopic observation of separate resonances for free and bound micelles at low temperature. Combining the ^{19}F NMR results with other detailed information derived from previous ^1H NMR, surface tension, viscosity, and conductometric studies, a structural model for the micelle–polymer supramolecular aggregates has been formulated.

Introduction

Over the past years a number of researchers have made extensive investigations concerning the physical chemical properties and the modification of the structures of both polymer and micellar aggregates in a variety of systems.^{1–4} Notwithstanding such a large effort, the detailed structure of the polymer–micelle assemblies has not yet been completely clarified.

Very recently, lithium heptadecafluorononanoate, LiPFN, in aqueous solutions of poly(vinylpyrrolidone), PVP, have been widely investigated in our laboratory.^{5–7} Data on the macroscopic properties (i.e., surface tension, viscosity, density, conductance) confirm that PVP favors the amphiphile aggregation, which occurs at a critical aggregation concentration of surfactant, CAC, much lower than the critical micellar concentration, CMC, observed in pure water. It has been also pointed out that the surfactant self-aggregation and the linkage of micelles to pyrrolidonic functional groups of the polymer are correlated processes.¹ ^1H NMR measurements^{5,6} have shown, in addition, that the polymer–surfactant interactions promote the stiffening of PVP.

In polymer–surfactant systems containing perfluorinated surfactants, the lack of hydrogen atoms on the hydrocarbon moiety

of the surfactant allows one to use ^1H and ^{19}F NMR measurements to investigate, separately, the structural changes of the polymer and of the surfactant occurring in the micelle–polymer aggregation process. In this paper, ^{19}F NMR measurements on LiPFN/PVP/water systems are presented and discussed. These results, integrated with the previous one obtained by ^1H NMR and macroscopic techniques^{5–7} provide an almost complete picture of the inter- and intramolecular interactions between the polymer and the lithium perfluorinated micelles and allow us to formulate a suitable model for these supramolecular aggregates.

Experimental Section

A. Material. Lithium Perfluorononanoate, LiPFN, was synthesized and purified according to the procedure already described.⁵ The product was vacuum-dried at 80 °C for 3 days before use. Poly(vinylpyrrolidones), PVP, Fluka products of different molecular weight, labeled as K30 and K90 were purified by dialysis to remove ionic impurities. Molecular weight determination of the used PVP has been obtained by gel-filtration chromatography. The PVP K90 sample gives a weighed average molecular weight $M_w = 428\,000$, a numerical average molecular weight $M_n = 139\,400$, and a polydispersity $P = 3.07$; the PVP K30 sample gives $M_w = 36\,200$, $M_n = 10\,650$, and $P = 3.40$.

* Corresponding author.

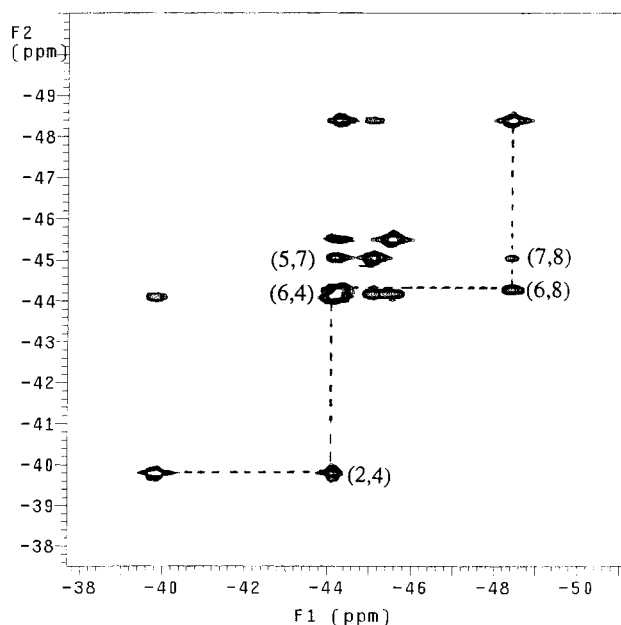


Figure 1. Expanded 470 MHz 2D COSY map showing ^{19}F – ^{19}F spin connectivities within the CF_2 region. CF_3 resonances not shown.

All solutions were prepared in deuterium oxide (Merck product 99.9% of purity).

B. Methods and Apparatus. The gel-filtration chromatography has been carried out using a Varian HPLC (model 5000) with TSK PWxl Toso Haas columns. The apparatus was calibrated by using pullulans as the standard.

In the ^{19}F NMR measurements on LiPFN/PVP/ D_2O systems, the concentration of PVP has been kept constant (1% w/w) while variable amounts of surfactant (from 10^{-6} to 10^{-1} mol kg^{-1}) were added. All solutions were prepared by weight.

^{19}F NMR spectra were recorded by a Varian Unity INOVA 500 spectrometer equipped with pulse field gradient module (Z axis) using a 5 mm Varian inverse probe with the high-band coil tuned at 470.302 MHz (^{19}F resonance). The ^{19}F 1D spectra were recorded in the range from +22 to –148 ppm using a 80 kHz spectral window (digitized points = 32K; 90° pulse = 8.1 ms; relaxation delay = 2 s).

N-type gradient-enhanced absolute-value COSY experiments were carried out using f_1 and f_2 spectral widths of 47 kHz, with rectangular gradient pulses of 2.0 ms in duration and approximately 3 G cm^{-1} strength (4K data points in the f_2 dimension; 512 time increments in f_1 , zero-filled to 1K; sin-bell weighting along both dimensions; 2 s delay). A single transient per increment was collected in concentrated solutions; otherwise, the number of scans was adjusted in relation to the sample dilution.

C. Assignment of the ^{19}F NMR Spectrum. ^{19}F NMR spectra of highly fluorinated hydrocarbons have been recently assigned by means of 2D homocorrelated ^{19}F – ^{19}F and hetero-correlated ^{13}C – ^{19}F maps.⁸ Following this assignment, strong J_{FF} coupling occurs mostly between groups separated by four bonds while vicinal coupling is near to zero, accordingly to data observed on fluoropolymers.⁹ COSY spectra must be read following the above observation, i.e., the experimental strong cross-peak must be $9 \div 7$, $8 \div 6$, $n \div n-2$ (see Figure 1). The resonance of the $-\text{CF}_3$ group has been assigned on the basis of intensity and chemical shift considerations. Starting from this group, the connectivity of the other ^{19}F resonances was performed from 2D COSY-90 maps.¹⁰

The obtained assignments (ppm) for LiPFN in D_2O (extrapolated at infinite dilution and relative to an external standard of CF_3COOH) are

$$^9\text{CF}_3 - ^8\text{CF}_2 - ^7\text{CF}_2 - ^6\text{CF}_2 - ^5\text{CF}_2 - ^4\text{CF}_2 - ^3\text{CF}_2 - ^2\text{CF}_2 - ^1\text{COO}^-$$

ppm –3.01 –48.25 –44.94 –44.14 –44.01 –44.01 –45.42 –39.71

The occurrence of the surfactant–polymer interactions and the formation of the micellar assemblies causes strong variation of the chemical shifts. Thus, when necessary, COSY 2D maps have been repeated allowing the assignment reported in Table 1 and 2.

Results and Discussion

A. LiPFN– D_2O System. The dependence of all ^{19}F chemical shifts as a function of the natural logarithm of the surfactant molality, m , is shown in Figure 2a–h.

As can be observed for the LiPFN/water systems (identified in the figure with empty circles), the plots exhibit the typical features of most amphiphilic compounds with a flat trend at lower concentrations, followed by a sudden upfield shift at higher concentrations. The well-defined break point, occurring in all plots at the same surfactant concentration $8.8 \pm 0.2 \times 10^{-3}$ mol kg^{-1} , is due^{11–14} to the surfactant critical micellar concentration, CMC.

As shown in Table 3, the value of CMC found by ^{19}F NMR is in agreement with the values obtained by macroscopic techniques.^{5,6} As previously pointed out,⁷ slight discrepancies of the CMC values, in particular that obtained by conductance data, can be attributed to the different phenomena on which the various methodologies are based.

According to Pople et al.,¹⁵ the occurrence of a chemical shift during the micellization process can be explained as due to a variation of the local dielectric constant. As shown in Table 1, such interpretation is fully supported by the sequence of the magnitude of chemical shift variations, $\Delta\delta$, obtained in our system

$$\Delta\delta \quad \Delta\delta \quad \Delta\delta \quad \Delta\delta \quad \Delta\delta \quad \Delta\delta \quad \Delta\delta \quad \Delta\delta$$

$$^9\text{CF}_3 > ^8\text{CF}_2 > ^7\text{CF}_2 > ^6\text{CF}_2 \geq ^5\text{CF}_2 > ^4\text{CF}_2 > ^3\text{CF}_2 \geq ^2\text{CF}_2$$

the results of which correlated with the distance between the carbons bearing the fluorine atoms and the LiPFN headgroup. Note that the $-\text{CF}_3$ group located at the end of the surfactant hydrophobic chain is the most sensitive to the dielectric constant changes of the environment surrounding the LiPFN molecules passing from the aqueous solution to the hydrophobic micellar core during the micellization process.

It has been hypothesized^{16–18} that in the micellization process, the surfactant molecules undergo to a conformational variation. Such a hypothesis does not hold in our systems. As shown in Table 1, in fact, passing from the free monomers to micelles, we observe a continuous trend of the chemical shift of all the fluorine atoms bound to the different carbons instead of any strong chemical shift variation¹⁹ that should be induced by the presence of any form of g - g turn.

Additional information on the micellization process can be obtained analyzing the variation of the line width as a function of the surfactant concentration. The ^{19}F NMR spectra show, in fact, a small broadening for all fluorine atoms linked to the different carbon atoms of the LiPFN molecule above the CMC. As an example, the results obtained for the fluorine atoms linked to the carbon in position 9 are reported in Figure 3 (curve with empty circles). The observed broadening can be interpreted in

TABLE 1: Chemical Shifts, δ (ppm), of Fluorine Bound to the Different Carbon Atoms of LiPFN at Different Surfactant Concentrations, m (mol Kg⁻¹), for the LiPFN/Water System

$10^3 m$	δC_2	δC_3	δC_4	δC_5	δC_6	δC_7	δC_8	δC_9
0.0827	-39.71	-45.42	-44.01	-44.01	-44.14	-44.94	-48.25	-3.01
0.2240	-39.71	-45.42	-44.02	-44.02	-44.14	-44.92	-48.25	-3.01
0.6560	-39.71	-45.42	-44.01	-44.01	-44.14	-44.94	-48.25	-3.01
0.8938	-39.71	-45.42	-44.02	-44.02	-44.14	-44.94	-48.25	-3.01
2.288	-39.71	-45.44	-44.02	-44.02	-44.14	-44.94	-48.26	-3.02
5.353	-39.71	-45.43	-44.02	-44.02	-44.15	-44.94	-48.26	-3.02
8.826	-39.71	-45.43	-44.03	-44.08	-44.15	-44.95	-48.27	-3.02
11.11	-39.73	-45.44	-44.06	-44.09	-44.19	-44.99	-48.33	-3.10
14.98	-39.90	-45.58	-44.40	-44.45	-44.58	-45.42	-48.88	-3.82
15.76	-39.91	-45.48	-44.40	-44.45	-44.59	-45.43	-48.89	-3.84
20.86	-39.98	-45.63	-44.53	-44.75	-44.65	-45.61	-49.10	-4.11
133.0	-40.25	-45.82	-45.07	-45.26	-45.31	-46.27	-49.96	-5.28
199.9	-40.26	-45.79	-45.09	-45.26	-45.34	-46.28	-50.01	-5.34
219.6	-40.26	-45.81	-45.10	-45.29	-45.34	-46.29	-50.01	-5.36

TABLE 2: Chemical Shifts, δ (ppm), of Fluorine Bound to the Different Carbon Atoms of LiPFN at Different Surfactant Concentrations, m (mol Kg⁻¹), for the LiPFN/Water/PVP Systems

$10^3 m$	δC_2	δC_3	δC_4	δC_5	δC_6	δC_7	δC_8	δC_9
PVP K 90								
0.5659	-39.26	-45.10	-44.31	-44.44	-44.56	-45.42	-48.90	-3.82
02.164	-39.15	-45.01	-44.41	-44.57	-44.71	-45.59	-49.11	-4.16
5.285	-39.04	-44.91	-44.55	-44.72	-44.91	-45.78	-49.37	-4.51
16.75	-39.10	-49.91	-44.65	-44.80	-44.91	-45.90	-49.56	-4.82
39.70	-39.48	-45.10	-44.83	-44.83	-45.10	-45.94	-49.65	-4.96
189.9	-40.10	-45.62	-45.28	-45.28	-45.28	-46.25	-49.99	-5.35
PVP K 30								
0.1137	-39.60	-45.33	-43.99	-43.99	-43.99	-44.91	-48.23	-2.98
0.1839	-39.59	-45.33	-43.99	-43.99	-43.99	-44.91	-48.23	-2.98
0.5770	-39.54	-45.30	-43.04	-43.04	-43.04	-45.00	-48.32	-3.08
1.009	-39.39	-45.20	-44.22	-44.22	-44.22	-45.20	-48.62	-3.51
1.244	-39.30	-45.07	-44.46	-44.46	-44.46	-45.55	-49.11	-4.25
2.527	-39.10	-44.98	-44.44	-44.59	-44.74	-45.61	-49.15	-4.24
7.637	-39.03	-44.91	-44.58	-44.75	-44.91	-45.82	-49.44	-4.61
21.82	-39.20	-44.96	-44.69	-44.83	-44.96	-45.93	-49.62	-4.90
38.44	-39.47	-45.09	-44.75	-44.86	-45.09	-45.97	-49.68	-4.99
153.4	-40.06	-45.60	-45.03	-45.17	-45.28	-46.24	-49.97	-5.32
187.4	-40.11	-45.63	-45.06	-45.21	-45.31	-46.26	-50.00	-5.36

TABLE 3: Critical Micellar Concentrations of LiPFN in Water Obtained with Different Techniques

technique	10^3CMC
¹⁹ F NMR	8.8
surface tension	8.2
viscosity	8.7
conductivity	10.8

terms of a fast exchange between a sharp resonance due to the monomers (average value 8 ± 2 Hz) and a slightly broader resonance due to the micelles (average value 28 ± 5 Hz).

B. LiPFN–D₂O–PVP Systems. For the sake of clarity, let us divide the discussion of LiPFN–D₂O–PVP systems by separately analyzing three different surfactant concentration ranges, namely the first up to 6×10^{-4} mol kg⁻¹, the second between 6×10^{-4} and 1.8×10^{-2} mol kg⁻¹, and the highest concentration range above 1.8×10^{-2} mol kg⁻¹.

As shown in Figure 2, up to a LiPFN concentration of 6×10^{-4} mol kg⁻¹ the trend of the resonance curves does not depend on the polymer molecular weight and remains flat for the majority of fluorine atoms linked to different carbons of the surfactant molecule. However, inspection of Figure 2a and 2b reveals that the presence of a polymer in solution causes a downfield variation of the chemical shift of the fluorine atoms bound to the carbons nearest neighbor to the surfactant headgroup (i.e., C2 and C3) of about 0.11 and 0.09 ppm, respectively, with respect to the LiPFN–D₂O system. Since, as previously found,^{5,7} in such a concentration range the LiPFN molecules are in the monomeric state, the result can be

rationalized assuming that significant interactions between the two solutes (i.e., LiPFN and PVP) exist and a dynamic equilibrium between free LiPFN monomers and LiPFN monomers linked to a PVP backbone is established in solution.

Concerning the line width behavior, Figure 3 shows that up to a surfactant concentration of 6×10^{-4} mol kg⁻¹, the results obtained for the LiPFN–PVP–water systems exactly match those observed for the binary LiPFN–water system.

We consider next the results obtained in the middle concentration range (6×10^{-4} to 1.8×10^{-2} mol kg⁻¹). Analyzing Figure 2 we note that just above the LiPFN concentration equal to 6×10^{-4} mol kg⁻¹, previously assumed^{5,6} as the critical association concentration, CAC, of our system, the chemical shifts of the fluorine atoms linked to the carbons from position 4–9 (i.e., distant from the surfactant headgroup) display a significant upfield shift (see Figures 2c–h), not depending on the polymer molecular weight. According to the considerations previously given to explain the similar behavior in pure water, just above CMC, the upfield shift in LiPFN–PVP–water systems can be attributed to the micellization process at the CAC point.

For ionic surfactants interacting with a polar polymer, the lowering of the surfactant self-aggregation process at the CAC point, besides the effect due to the participation of the polymer in the air–water interface, has been generally attributed to the decrease of repulsive forces between the charged headgroups caused by the polar group of the polymer surrounding the surfactant assemblies. Apart from these effects, other additional

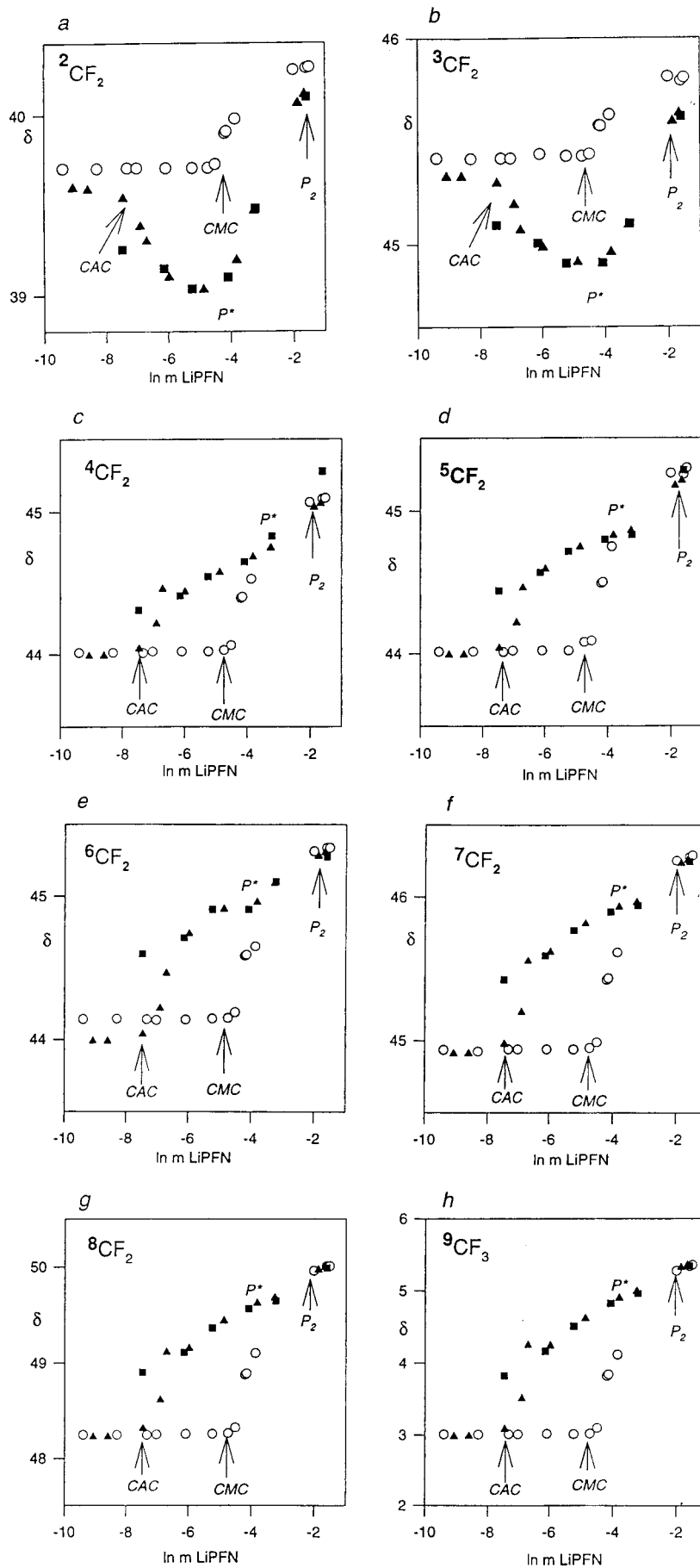


Figure 2. Chemical shifts (δ) for the different fluorine atoms against the natural logarithm of the surfactant concentration, $\ln m$. LiPFN/water system (○), LiPFN/PVP K30/water system (▲), LiPFN/PVP K90/water system (■).

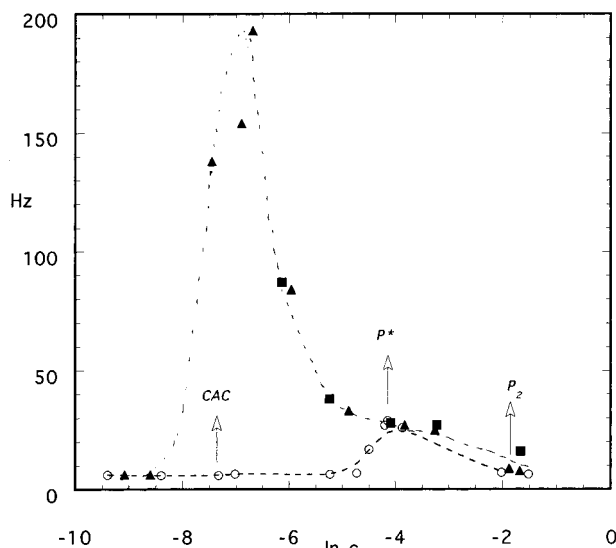


Figure 3. Line width, λ , of the ^{19}F resonances of CF_3 as a function of the surfactant concentration in water (○), in PVP K30/water (▲), and in PVP K90/water (■). The lines in the figure represent a guide for visual comparisons.

contributions can effect the phenomenon. Among them, according to the “tube model” used to describe the polymer dynamics²⁰ in solution, we should consider that around each macromolecule there is a narrow region containing the water molecules belonging to the first solvation shells^{21–22} of polymer. Under these circumstances, the number of water molecules in which the surfactant is dissolved is decreased (in other words the “real” concentration of the surfactant becomes greater than the stoichiometric one), thus a contribution to the anticipation of the CMC at the CAC point promoted by the presence of the polymer in the bulk may be forwarded.

A perusal of Figure 2 shows that between 6×10^{-4} and $1.8 \times 10^{-2} \text{ mol kg}^{-1}$ of LiPFN, the ^{19}F chemical shift for the fluorine atoms linked to the carbons from position 4–9 regularly increases; it is scarcely influenced by the polymer molecular weight and it approaches the values obtained for the LiPFN–water system at a LiPFN concentration around $P^* = 1.8 \times 10^{-2} \text{ mol kg}^{-1}$. In view of our previous surface tension, viscosity, volume, and ^1H NMR results,^{5–7} such a behavior can be rationalized considering that in this concentration range the binding sites of the polymer become saturated by LiPFN micelles.

As can be seen in Figure 2a and 2b, the behavior of the chemical shift of the fluorine atoms linked to C2 and C3 (i.e., close to the surfactant polar head) is completely different. Just above the CAC the chemical shift undergoes, in fact, a downfield shift, reaches a minimum at P^* , and thereafter moves upfield to approach the values of the LiPFN–water systems.

It has been previously postulated, on the basis of conductometric⁷ and ^1H NMR results,^{5,6} that micelle–polymer interactions occur between the charged headgroup of LiPFN and the polar sites, $-\text{N}^+=\text{C}-\text{O}^-$, of the PVP. Thus, the particular behavior of the chemical shift of fluorine atoms linked to C2 and C3 can be rationalized in terms of charge effects²³ due to the charge redistribution near to the surfactant polar headgroup.

The behavior of the line width in the surfactant concentration range 6×10^{-4} to $1.8 \times 10^{-2} \text{ mol kg}^{-1}$ presents some peculiarities that give useful information on the dynamics of the systems. In particular, we observe in Figure 3 that the line broadening for the resonance of the CF_3 group increases above the CAC from 6 to 193 Hz thereafter decreases to the values of the LiPFN–water system at the saturation concentration P^* .

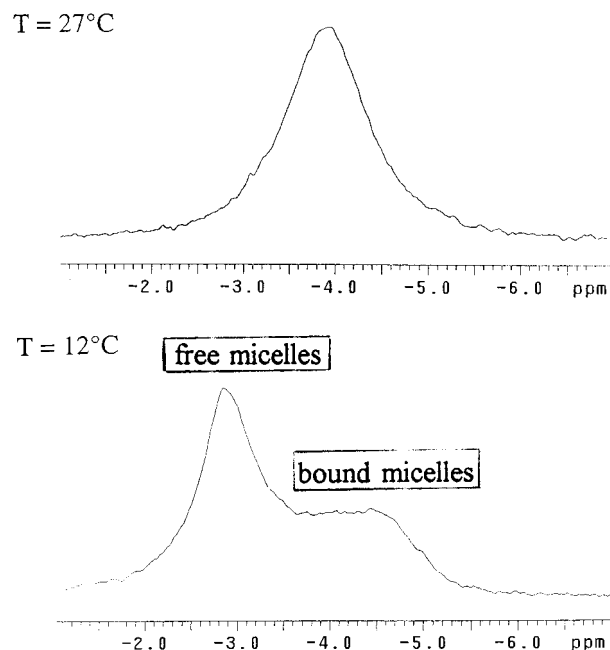
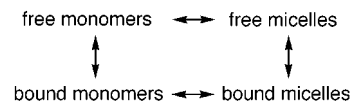


Figure 4. ^{19}F NMR spectrum of the LiPFN/water/PVP K30 ($1.244 \times 10^{-3} \text{ mol kg}^{-1}$) system. Only the CF_3 region is shown at 27 (top line) and at 12 °C (bottom line), respectively.

A rationalization of this behavior can be obtained²⁵ taking into account the presence of the following chemical equilibrium.



As can be observed from Figure 3 at low surfactant concentrations (well below the CAC) where the only equilibrium between the free LiPFN monomers and the LiPFN monomers bound to PVP can be postulated, the line widths are practically coincident to the values obtained in the binary LiPFN/water systems. Such a coincidence indicates that the free monomers \leftrightarrow bound monomers equilibrium must occur with an exchange rate faster than the NMR observation, thus its contribution in the observed line broadening can be ignored. Concerning the equilibrium between free LiPFN monomers and LiPFN micelles, it has been shown (see the discussion on LiPFN–water system) that it is characterized by the sharp resonance of the monomers (8 Hz), and the slightly broader resonance of micelles (20 Hz), thus also contributes to this equilibrium to the broadening of CF_3 observed in the LiPFN concentration range between 6×10^{-4} and $1.8 \times 10^{-2} \text{ mol kg}^{-1}$, can be neglected.

In view of the above consideration, the large broadening of the CF_3 resonance must be attributed to the equilibrium between free micelles and polymer-bound micelles with the assumption that it occurs with an exchange rate comparable to the NMR observation time.

To prove this assessment, additional ^{19}F NMR measurements on the LiPFN–PVP(K30)–water system have been performed at 12 °C. The results, reported in Figure 4, showing a clear splitting of the CF_3 resonance and a ratio of bound micelles/free micelles of approximately 1:1, confirm our hypothesis.

We finally consider the results in the higher concentration range (above $1.8 \times 10^{-2} \text{ mol kg}^{-1}$). As shown in Figure 2, the chemical shift for the LiPFN–PVP–water systems is quite similar to the binary LiPFN–water system. This feature can be rationalized taking into account that at high concentration

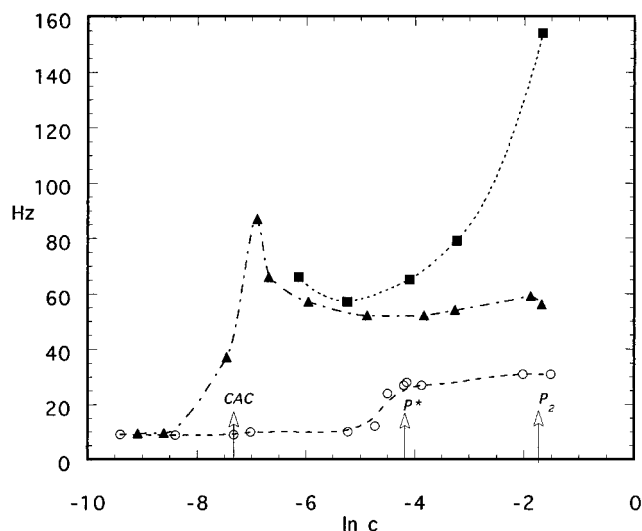


Figure 5. Line width, λ , of the ^{19}F resonances of $^{2}\text{CF}_2$ as a function of the surfactant concentration in water (○), in PVP K30/water (▲), and in PVP K90/water (■). The lines in the figure represent a guide for visual comparisons.

(i.e., P_2), after polymer saturation, the free micelles become the dominant species in solution.

Above $1.8 \times 10^{-2} \text{ mol kg}^{-1}$ LiPFN, the line width behavior of fluorine atoms linked to the different carbons of the surfactant molecules shows some peculiarities which deserve some comments. Apart from data relative to the CF_3 group (Figure 3), whose intrinsic line width is dominated by the internal rotation, all other resonances are rather broad and become sensitive to the polymer molecular weight (Figure 5 represents, as an example, the broadening of the line width of $^{2}\text{CF}_2$). Such features, reflecting the broadening of the resonance peaks of ^1H spectra previously reported,^{5,7} can be rationalized assuming the presence of a fast equilibrium between different species in which at least one (i.e., bound micelles) has a large value of the intrinsic line width.

C. Structural Model for LiPFN–PVP Supramolecular Aggregates. A model based on the penetration of polymer segments into the micellar core has been proposed by different authors^{28,29} to represent the supramolecular polymer–surfactant aggregates. Strong experimental evidence obtained for the LiPFN–PVP systems indicate that, at least for this systems, such a model can be rejected. The lack of separated chemical shift for ^{19}F nuclei after the polymer saturation, the unobserved ^{19}F – ^1H NOE,^{26,27} and the difference in the line width between ^1H spectra of the polymer and ^{19}F spectra of micelles are some of the evidence against the above model.

Considering the results previously collected in our laboratory^{5–7} together with the ^{19}F NMR results so far discussed, a realistic model in which the polymer chain might wrap one or more micellar structures to form a sort of *dressed micelles*³⁰ can be proposed to represent the LiPFN–PVP aggregates (see Figure 6). For long-chain polymers (high molecular weight), the supramolecular aggregates polymer–micelles should be particularly rich in micelles distributed along the polymer chain to account for the high polymer stiffening pointed out by the ^1H NMR results and for the high viscosity of the system. On the other hand, for low molecular weight polymers, the micelles population along the polymer chain should be reduced in order to account for the observed flexibility of the polymer and for the moderate viscosity of the system.⁶

Some rough calculations, carried out for the polymers at different molecular weight, can give the possible stoichiometry

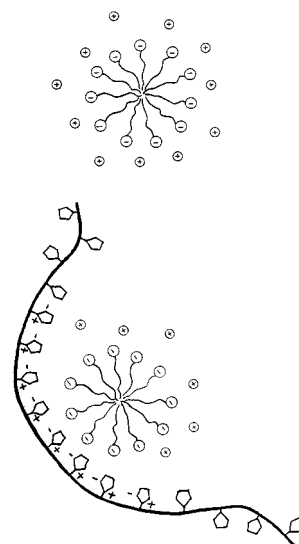


Figure 6. Proposed model for the LiPFN–PVP supramolecular structure.

of the polymer–micelles aggregates. The monomeric vinylpyrrolidonic groups, PV, in 1% PVP solutions, are about 0.0909 mol/kg. Thus, at the CAC ($\approx 6 \times 10^{-4} \text{ mol/kg}$), the ratio between the LiPFN and PV groups is 1:151. It increases up to 1:8 when the surfactant concentration reaches P^* ($\approx 1.1 \times 10^{-2} \text{ mol/kg}$). Assuming for the LiPFN micelles an average aggregation number $N \approx 12$ –20 surfactant molecules^{31,32} and considering that the polymer partially envelopes the micellar assembly (only an emicircumference is interested in the polymer–surfactant interactions), we can estimate that the micelles randomly distributed along the polymer backbone are separated at least by 90–100 vinylpyrrolidonic groups. This means that in the case of PVP–K90 ($M_w = 428\,000$ and $\sim 3850 \pm 50$ vinylpyrrolidonic groups per molecule), each polymer chain links about 40–50 micelles, whereas for the lower molecular weight polymer, for example PVP–K30 ($M_w = 36\,200$ and ~ 320 –330 vinylpyrrolidonic groups), the number of micelles linked to the polymer is reduced to ~ 4 units.

Acknowledgment. Acknowledgment is due to the Ministero dell'Università e della Ricerca Scientifica (Cofin. MURST 97 CFSIB) for financial support. All the ^{19}F NMR spectra have been performed at Chemistry Department, Catania University.

References and Notes

- (1) Lindman, B.; Karlstrom, G. In *The structures and Equilibrium Properties of Colloidal Systems*; Bloor, D. M., Wyn-Jones, E., Eds.; Kluwer Academic: Dordrecht, The Netherlands, 1990; p 131.
- (2) Goddard, E. D. *Interaction of Surfactant with polymers and proteins*; Goddard, E. D., Ananthapadmanabhan, K. P., Eds.; CRC Press: Boca Raton, FL, 1993.
- (3) Saito, S. P. In *Non Ionic Surfactant*; Schick, M. J., Ed.; Marcel Dekker: New York 1987; p 881.
- (4) Hayakawa, K.; Kwak, J. C. T. In *Cationic Surfactant*; Rubing, D. N., Holland, P. M., Eds.; Marcel Dekker: New York, 1991; p 189.
- (5) Sesta, B.; Segre, A. L.; D'Aprano, A.; Proietti, N. *J. Phys. Chem.* **1997**, *101*, 198.
- (6) Sesta, B.; Segre, A. L.; D'Aprano, A.; Proietti, N. *Langmuir* **1997**, *13*, 6612.
- (7) D'Aprano, A.; Sesta, B.; Proietti, N.; Mauro, V. *J. Solution Chem.* **1997**, *26*, 649.
- (8) Ribeiro, A. A. *Magnetic Resonance in Chemistry* **1997**, *35*, 215.
- (9) Ovenall, D. W.; Ferguson, R. C. *Pulse Methods in 1D and 2D Liquid-Phase NMR*; Brey, W. S., Ed.; Academic Press: San Diego, 1987.
- (10) Braun, S.; Kalinowski, H. O.; Berger, S. *100 and more basic NMR experiments*; VCH Publisher: Weinheim, Germany, 1996.
- (11) Wennerstrom, H.; Lindman, B.; Soderman, O.; Drakenberg, T.; Rosenholm, J. *J. Am. Chem. Soc.* **1979**, *101*, 6860.

- (12) Drakenbert, T.; Lindman, B. *J. Colloid Interface. Sci.* **1973**, *44*, 184.
- (13) Soderman, O.; Lindman, B.; Stilbs, P. In *Nuclear Magnetic Resonances*; Webb, G. A., Ed.; London, 1983; Vol. 12, p 302.
- (14) Soderman, O. In *Nuclear Magnetic Resonances*; Webb, G. A., Ed.; London 1983; Vol. 14, p 350.
- (15) Pople, J. A.; Schneider, W. G.; Bernstein H. J. *High-resolution Nuclear Magnetic Resonance*; McGraw-Hill: New York, 1959.
- (16) Mazer, N. A.; Benedeck, G. B.; Carey, M. C. *J. Phys. Chem.* **1976**, *80*, 181.
- (17) Ninnham, B. W. *J. Phys. Chem.* **1979**, *84*, 1423.
- (18) Dill, K. A.; Flory, P. J. *Proc. Natl. Acad. Sci.* **1981**, *78*, 676.
- (19) Tonelli, A. E. *NMR Spectroscopy and Polymer Microstructure. The Conformational Connection*; VCH Publishers, Inc.: New York, 1989.
- (20) Doi, M.; Edwards, S. F. In *The Theory of Polymer Dynamics*; Oxford University Press: New York, 1986; p 207.
- (21) Derbyshire, W.; Duff, I. D. *Discuss. Faraday Soc.* **1974**, *57*, 243.
- (22) Quinn, F. X.; Kampft, E.; Smyth, G.; McBrierty, V. J. *Macromolecules* **1988**, *21*, 3191.
- (23) Saika, A.; Slichter, C. P. *J. Chem. Phys.* **1954**, *26*, 968.
- (24) Kaplan, J. J.; Fraenke, G. A. *NMR of Chemically Exchanging Systems*; Academic Press: New York, 1980.
- (25) Ernst, R. R.; Bodenhausen, G.; Wokaun, A. *Principles of Nuclear Magnetic Resonance in One and Two Dimensions*; Clarendon Press: Oxford, 1987; Chapter 2, p 63.
- (26) Unpublished data.
- (27) Neuhaus, D.; Williamson, M. *The Nuclear Overhauser effect*; VCH Publisher: Weinheim, Germany, 1956.
- (28) Turro, N. J.; Lei, X.; Ananthapadmanabhan, K. P.; Aronson, M. *Langmuir* **1995**, *11*, 2525.
- (29) Guo, X. H.; Zhao, N. M.; Chen, S. H.; Texeira, J. *Biopolymers* **1990**, *29*, 335.
- (30) Nagarajan, R.; Kalpakci, B. *Polym. Prepr.—Am. Chem. Soc., Div. Polym. Chem.* **1982**, *23*, 41.
- (31) La Mesa, C.; Sesta, B. *J. Phys. Chem.* **1987**, *91*, 1450.
- (32) Kissa, E. In *Fluorinated Surfactants: Synthesis, Properties, Applications*; Kissa, E., Ed.; Marcel Dekker Inc.: New York, 1993; Chapter 8.